# Sodium Ion Apparent Diffusion Coefficient in Living Rat Brain

James A. Goodman,[1] Christopher D. Kroenke,[2] G. Larry Bretthorst,[2] Joseph J. H. Ackerman,[1,2,3] and Jeffrey J. Neil[2,4]*

**The apparent diffusion coefficient (ADC) of $Na^+$ was determined in live rat brain. The brain extracellular-to-intracellular $Na^+$ content ratio is ~8:2, which is the inverse of that for water in these spaces. Consequently, the ADC of $Na^+$ is primarily affected by motion in the extracellular space, and $Na^+$ can be viewed as a reporter molecule for motion in that space. Likewise, water ADC is dominated by intracellular motion. The brain $Na^+$ ADC was 1.15 ± 0.09 $\mu m^2$/ms, which is 61% of the aqueous $Na^+$ free diffusion coefficient ($D^{free}$) at 37°C (1.9 $\mu m^2$/ms), while the ADC for brain water is 28% of the water $D^{free}$ at 37°C (3 $\mu m^2$/ms). This suggests that the ADC of molecular species within the extracellular space is roughly twofold that within the intracellular space. In postmortem brain, both $Na^+$ and water decrease to 17% of the respective $D^{free}$ values. These results are consistent with $Na^+$ and water ADC values sharing the same biophysical determinants in postmortem brain. The observed difference between $Na^+$ and water ADC/$D^{free}$ ratios in living brain tissue may be attributable to the extracellular environment hindering molecular displacements twofold less than the intracellular environment. Magn Reson Med 53:1040–1045, 2005. © 2005 Wiley-Liss, Inc.**

**Key words: in vivo MRS; Na NMR; sodium diffusion; compartmental diffusion; brain**

The rate constant governing water incoherent displacement in tissue, the apparent diffusion coefficient (ADC), decreases markedly following various injuries to brain tissue (1–6). Although this phenomenon is exploited daily in the clinical setting to detect injury via diffusion-weighted images, the underlying biophysical mechanisms that cause the water ADC to change are not comprehensively understood. Characterization of water incoherent displacement motion in the intra- and extracellular compartments following injury would provide an important advance toward the elucidation of these mechanisms. Unfortunately, resolution of the water MR signal in each of these two compartments in the CNS remains a difficult problem, although progress toward this goal has been reported (7,8).

One strategy for making inferences about the motion of the water in each of these compartments is to employ endogenous or exogenous MR-active chemical species (ions and molecules) that are present in the aqueous phase of either or both spaces and that can be compartmentally distinguished. The sodium ion is potentially one such species. In the normally functioning central nervous system, as in virtually all tissues, significant amounts of intracellular and extracellular sodium ion are present, and the concentration gradient across the plasma membrane is held fixed. The sodium ion concentration is roughly 140 mM (9) and 10 mM (10) in the extracellular and intracellular spaces, respectively. Since the extracellular space comprises about 20% of brain volume (9), there are about 3.5 times more sodium ions in the extracellular compartment than there are in the intracellular compartment. Thus, roughly 80% of the $^{23}Na$ MR signal (assuming similar $T_1$ and $T_2$ relaxation times in both compartments) is from the extracellular space, making the sodium ion an endogenous, compartment selective (although not entirely compartment specific) marker of the extracellular space. For this reason, we have developed a method for determining the ADC of total tissue sodium ("bulk" sodium) in rat brain.

Many technical challenges must be overcome to perform in vivo diffusion measurements of tissue sodium ions by $^{23}Na$ MR. First, $^{23}Na$ has a magnetogyric ratio, $\gamma$, that is about one fourth that of the $^1H$ nuclide. As a result (vide infra), much stronger (~16×) diffusion encoding magnetic field gradients are required relative to those employed for $^1H$ MR water diffusion measurements. Second, the brain bulk sodium ion concentration is about 40 mM, much less than the ~80 M $^1H$ concentration of tissue water. Thus, to achieve an acceptable signal-to-noise ratio for quantifying the MR signal amplitude, the average of many signal transients is needed. Third, $^{23}Na$ is a quadrupolar nucleus, resulting in a short transverse relaxation time constant, $T_2$, of about 34 ms. (A second $T_2$ component, related to the presence of multiple quantum coherences, has also been observed and is characterized by a ~5-ms $T_2$. In the experiments described below, this "fast component" has fully decayed and does not comprise a significant fraction of the signal.) These three factors require the echo time to be minimized, the diffusion gradient strength to be maximized, and the repetition time of the experiment to be short. These constraints on the MR experiment impose considerable demands on the spectrometer.

Because of these technical challenges, $Na^+$ diffusion has been studied using MR in only a small number of biologic systems. Van der Veen et al. (11) measured $Na^+$ diffusion in a sample containing red blood cells. By adjusting the diffusion time of the MR diffusion experiment, the authors

[1]Department of Chemistry, Washington University, St. Louis, Missouri, USA.
[2]Department of Radiology, Washington University, St. Louis, Missouri, USA.
[3]Department of Internal Medicine, Washington University, St. Louis, Missouri, USA.
[4]Department of Pediatric Neurology, Washington University, St. Louis Missouri, USA.

Grant sponsor: NIH; Grant numbers: NS35912 and R24-CA83060; Grant sponsor: Department of Education; Grant number: P200A00217.

*Correspondence to: Professor Jeffrey J. Neil, Biomedical MR Laboratory, Campus Box 8227, Washington University School of Medicine, East Building, 4525 Scott Avenue, St. Louis, MO 63110, USA. E-mail: neil@wustl.edu

Received 2 August 2004; revised 10 November 2004; accepted 12 November 2004.
DOI 10.1002/mrm.20444
Published online in Wiley InterScience (www.interscience.wiley.com).

were able to assess the effect of restriction due to the cell membrane upon the $Na^+$ ADC. Additionally, Sehy et al. (12) have measured the intracellular $Na^+$ ADC within a single *Xenopus* oocyte.

We have developed a technique for measuring $Na^+$ diffusion in rat brain in situ. These measurements employ a small, two-turn ellipsoidal surface radiofrequency transmit/receive coil (1.4-cm major axis, 1.0-cm minor axis), which sits directly on the rat's skull immediately above the brain. The coil's region of interrogation determines two dimensions of the region of interest. Slice-selective adiabatic RF pulses and magnetic field gradients were used to provide the third dimension of localization. The bulk brain $Na^+$ ADC in vivo was found to be $1.15 \pm 0.09$ $\mu m^2$/ms, which is 61% of the $Na^+$ diffusion coefficient ($D^{free}$) in temperature-matched dilute aqueous solution (13). In comparison, the brain water ADC is 28% of $D^{free}$. Upon death, the ADC values for both $Na^+$ and water drop to 17% of the respective $D^{free}$ values.

## MATERIALS AND METHODS

### Animal Preparation

All experimental procedures were performed in accordance with NIH guidelines and Washington University Institutional Animal Care and Use Committee regulations. Male Sprague–Dawley rats, 250–400 g, were anesthetized by intraperitoneal (i.p.) injection of 1.2 mL/100 g body wt 10% urethane solution. A booster of 0.6 mL/100 g body wt of the same solution was administered 30 min later. To minimize animal motion during the MR measurements, an MR-compliant head restraint device consisting of ear bars and a nose cone/bite bar was used. Heart rate and arterial oxygenation were monitored with a pulse oximeter (Nonin Medical, Plymouth, MN) attached to a hind paw. To maintain normal blood oxygenation levels under anesthesia, 100% $O_2$ gas was blown into the nose cone. Body temperature was maintained by circulating warm water through a heating pad on which the animal rested. In vivo body core temperature was monitored rectally with a fiber optic temperature probe (Fiso, Sainte-Foy, Québec, Canada), and brain temperature was monitored via $^1H$ MRS (vide infra). In postmortem studies, brain temperature was maintained by blowing warm air over the head while continuing circulation of warm water under the animal. A fiber optic temperature probe was placed in the nasal cavity to estimate brain temperature, as the spectroscopic measurement was less reliable in postmortem brain because of an increase in linewidth related to the presence of deoxyhemoglobin. Animals for postmortem study were euthanized in the magnet with a 1-mL bolus of 2 M KCl delivered via a catheter in the femoral vein.

### MR Experiments

Imaging and spectroscopy experiments employed an Oxford Instruments, 40-cm diameter (clear bore), 4.7-T magnet equipped with Magnex 10-cm (inner diameter), actively shielded gradient coils capable of producing linear magnetic field gradients of up to 60 G/cm with ~200 μs rise time. A Varian NMR Systems INOVA console controlled the magnet and gradient systems. Experiments were performed using a 4-cm, single-turn surface coil for

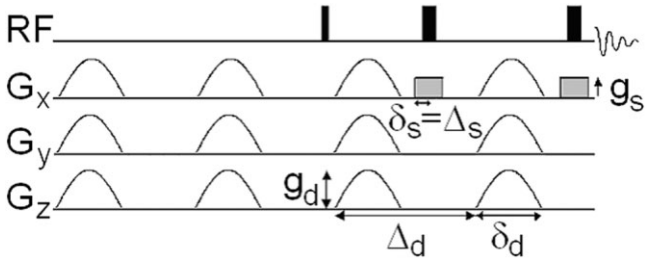


FIG. 1. The LASER pulse sequence modified with sine-shape gradient warm-up prepulses and diffusion-weighting pulses. The prepulses put the gradient system in a steady state, which enhances the reproducibility of the pulses. The first RF pulse is an adiabatic half-passage pulse, and the second two slice-selective RF pulses are adiabatic full-passage pulses. The second adiabatic full-passage pulse is required to rewind the nonlinear phase of the magnetization induced by the first adiabatic full-passage pulse.

$^1H$ measurements and a two-turn ellipsoidal surface coil of major and minor diameters of 1.4 and 1.0 cm, respectively, for $^{23}Na$ experiments. The $^1H$ coil was placed along the side of the animal's head, and the sodium coil was placed orthogonal to the $^1H$ coil, directly above the brain. The orthogonal arrangement of the coils minimized coupling between them.

After each rat was placed in the magnet, a series of $^1H$ MR control experiments was performed. Multislice, gradient-echo images, using a repetition time (TR) of 60 ms and an echo time (TE) of 6.5 ms, were acquired to guide the selection of a volume element for $^1H$ and $^{23}Na$ localized spectroscopy. Localized $^1H$ spectra were acquired using the localization by adiabatic selective refocusing (LASER) pulse sequence (14). Using a LASER sequence that is modified to include diffusion-sensitizing gradients (15), the $^1H_2O$ ADC was measured from 25 spectra obtained with the *b*-value parameter ranging from 0.1 to 2.5 ms/$\mu m^2$ in steps of 0.1 ms/$\mu m^2$ for living rats and 0.2 to 5.0 ms/$\mu m^2$ in steps of 0.2 ms/$\mu m^2$ for postmortem rats. The pulse sequence settings were TR = 1.76 s, TE = 75 ms, diffusion-sensitizing gradient pulse lengths of 5 ms, and separation between the gradient pulses of 50.4 ms. The chemical shift difference between the *N*-acetylaspartate methyl $^1H$ signal and the $H_2O$ singlet in these spectra was used to measure the brain temperature using the method of Corbett et al. (16).

For $^{23}Na$ MR experiments, localization of the signal to within the brain was accomplished along two dimensions through the physical size of the RF coil. Localization along the remaining spatial dimension, which corresponds to the rat dorsal/ventral axis, was performed using the adiabatic double spin echo experiment shown in Fig. 1 (14). The volume element selected by this pulse sequence is approximately cylindrical, with regions proximal to the surface coil (such as cortex) contributing more to the MR signal than distal regions (basal ganglia). The pulse sequence shown in Fig. 1 was used to measure the $^{23}Na^+$ ADC and $T_2$ relaxation time constant. An inversion pulse was added to the beginning of the sequence to measure $T_1$ relaxation time constant.

During $^{23}Na^+$ ADC measurements, the diffusion encoding gradient pulses are constrained to be short, due to the short $^{23}Na$ $T_2$, and strong, due to the low $^{23}Na$ magnetogyric ratio. As a consequence, magnetic field gradients as large as

50 G/cm were needed. Large amplitude pulsed field gradients induce physical vibrations and eddy currents, which are both detrimental to ADC measurements. To minimize these effects, the methods described by Price et al. (17) were adopted. These include utilization of sine-modulated diffusion-sensitizing gradient pulse shapes and "steady-state" gradient prepulses. Pulse sequence timings for the $Na^+$ ADC measurements of living (dead) rats were TR = 230 (250) ms, TE = 32.2 (41.1) ms, $\delta$ = 10.5 (15.0) ms, and $\Delta$ = 14.9 (19.9) ms. Amplitudes of MRS signals were obtained from 10 spectra acquired with diffusion-sensitizing gradients ranging from 5 to 50 G/cm, in steps of 5 G/cm. A typical set of resulting *b*-values (vide infra) ranged from 0.023 to 2.078 ms/$\mu m^2$ for living rats and from 0.060 to 5.787 ms/$\mu m^2$ for rats postmortem. The data were collected in an interleaved cyclic manner, recording and storing a single transient for each of the 10 *b*-values and then repeating this procedure 512 times. The net signal transient recorded for each *b*-value was thus averaged (added) over the entire 21-min total acquisition period such that any systematic errors were averaged over all of the *b*-values. This reduces errors in the estimation of the ADC.

Estimation of MR signal amplitudes and subsequent data processing steps were performed using the Bayesian Analysis Package in Varian's VNMR software (18). The sum of signal transients at a given *b*-value was modeled as an exponentially decaying sinusoid. The estimated amplitudes of these sinusoids, taken at various diffusion encoding gradient strengths, were then fit to the expression for diffusion-attenuated, pulsed-gradient spin echoes given by Stejskal and Tanner (19),

$$S(b) = S(0)e^{-b*\mathrm{ADC}}, \quad [1]$$

where the *b*-value is given by (20)

$$b = \gamma^2 \int_{t=0}^{T} \left( \int_{t=0}^{t} G(t')dt' \right)^2 dt, \quad [2]$$

in which $\gamma$ is the magnetogyric ratio of the nucleus being measured, $G(t')$ is the magnetic field gradient strength at time $t'$, and $T$ is the length of the pulse sequence. In the case of sine-modulated gradient pulses, Eq. [2] reduces to

$$b = \gamma^2 \left[ \frac{4}{\pi} g_d g_s \delta_d \delta_s \Delta_s + 2 {g_s}^2 \delta_s^2 \left( \Delta_s - \frac{\delta_s}{3} \right) + \frac{12}{\pi^2} {g_d}^2 \delta_d^2 \left( \Delta_d - \frac{\delta_d}{4} \right) \right], \quad [3]$$

in which $g_i$ and $\delta_i$ represent the peak strength and length of gradient *i*, and $\Delta_i$ is the intergradient spacing for gradient pair *i*, as shown in Fig. 1.

To measure $T_1$, an inversion-recovery experiment was performed. The adiabatic half-passage sampling pulse followed a 2- to 3-ms slice-selective adiabatic inversion pulse at 10 variable delay times, TI, ranging from 0 to 180 ms. Estimated amplitudes of the MR signals, obtained using the Bayesian analysis, were modeled to the inversion recovery expression

$$S(\mathrm{TI}) = S(\infty) + (S(0) - S(\infty))e^{-\mathrm{TI}/T_1}. \quad [4]$$

To measure the $T_2$, TE was set to 10 different values ranging from 10 to 136 ms by adjusting the length of the second echo in the dual echo experiment. Relaxation time measurements were acquired in 15–17 min using 256 transients per relaxation delay, and the data were fit to the expression

$$S(\mathrm{TE}) = S(0)e^{-\mathrm{TE}/T_2}. \quad [5]$$

In principle, multiple-quantum coherences could lead to deviations of the experimental data from Eqs. [4] and [5]; however, no such deviations were observed. The lack of evidence of multiple-quantum coherences is attributed to three conditions: (1) The population of $Na^+$ experiencing sufficiently slow reorientational dynamics to generate such coherences (21,22) is small compared to the dominant $Na^+$ population, which experiences rapid, isotropic motion and experiences a symmetric solvation sphere. (2) The preparation time is not optimal for the generation of triple-quantum coherences in the selected experimental conditions. (3) Because these measurements all employ the adiabatic double spin echo experiment (TE $\sim$ 32ms), the fast-relaxing components of triple quantum coherences will essentially have completely decayed before data acquisition commences (23). Also in principle, biases in the $Na^+$ nuclear orientations throughout the voxel could give rise to residual quadrupolar couplings and generate multiple-quantum coherences (21,24). So far we have been unable to observe even-ordered $Na^+$ coherences in rat brain under optimized experimental conditions (unpublished observations) and therefore these effects can be neglected for the current experiments.

The above experiments were performed on the group of rats using the following protocol: (i) Gradient echo $^1H$ images were acquired to select the voxel for $^1H$ and $^{23}Na$ localized spectroscopy. (ii) Localized $^1H$ spectra were obtained for purposes of shimming the magnetic field within the volume of interest and measuring the brain temperature. (iii) The ADC of $H_2O$ within the voxel was determined using localized $^1H$ spectroscopy. (iv) The ADC, $T_2$, and $T_1$ of $Na^+$ within the voxel were determined using localized $^{23}Na$ spectroscopy. (iv) A second localized $^1H$ spectrum was acquired to measure brain temperature.

Diffusion experiments were performed again 10 min following animal sacrifice. This time allows the sodium ion concentration to reach an equilibrium distribution within intracellular and extracellular compartments after death. Living and postmortem brain temperatures were maintained within a 2°C SD of 37°C as monitored spectroscopically or with a fiber optic temperature probe placed in the nasal cavity. While these methods are indirect and somewhat imprecise estimates of brain temperature, the effect of temperature changes on ADC values ($\sim$2.5% per °C (13)) is small compared with the uncertainty in the ADC estimates ($\sim$8%, vide infra). Thus, these approximations of brain temperature are sufficient to demonstrate that temperature variations did not play a significant role in the observed ADC changes. Spectroscopic temperature measurements were also performed before and after the in vivo diffusion measurements, and $T_1$ and $T_2$ values were measured in living and postmortem rat brain.

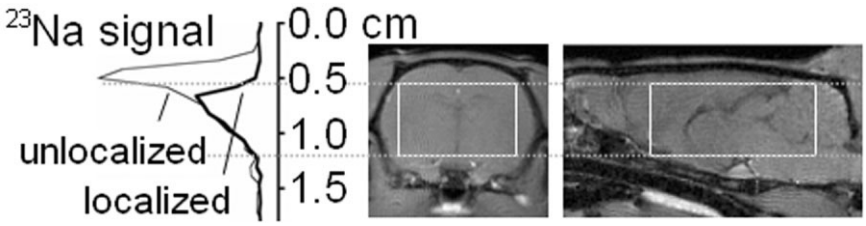


FIG. 2. Representative transaxial and sagittal images of rat brain. The thin line in the profile on the left represents data that result from applying a readout gradient in the vertical direction. The heavy line is the result of the same experiment except with the slice-select gradients turned on to localize the region shown in white boxes.

## RESULTS

For each subject, multislice, $T_2^*$-weighted, gradient-echo $^1$H images were used to select and display the volume of interest within the brain. Figure 2 shows representative coronal and sagittal views, respectively, from one rat. The rectangles in Fig. 2 delineate the approximate boundary of the target volume element for localized spectroscopy. Experimental verification that the observed $^{23}$Na MR signal originates almost completely from within the intended sample region is presented in Fig. 2. Two profiles of the $^{23}$Na MR signal are shown in the absence (thin line) and presence (thick line) of slice-selecting gradient pulses. Notably, signal from $Na^+$ within the blood and muscle of the scalp, which lie directly beneath the $^{23}$Na surface coil, is completely suppressed by the localization scheme.

Table 1 summarizes the results. Within a typical volume element of 0.8 mL, a mean signal-to-noise ratio obtained for the signal with $b = 0.023$ ms/$\mu$m$^2$ was 7. The near equivalence of the longitudinal and transverse relaxation times is consistent with $Na^+$ experiencing reorientational dynamics within the rapid isotropic tumbling regime, which is expected of solvated $Na^+$. The average ± average uncertainty of the individual $^{23}Na^+$ ADC values is 1.15 ± 0.09 $\mu$m$^2$/ms ($n = 18$), with an interanimal SD of 0.13 $\mu$m$^2$/ms. Following death, the $^{23}Na^+$ ADC dropped to 0.33 ± 0.07 $\mu$m$^2$/ms ($n = 7$), with an interanimal SD of 0.06 $\mu$m$^2$/ms. The $^{23}Na^+$ $T_1$ relaxation time constants for living and postmortem rats were measured to be 40 ± 4 and 35 ± 5 ms, respectively. The, $T_2$ relaxation time constants were 34 ± 2 and 30 ± 3 ms prior to and following sacrifice, respectively. Figure 3 displays representative data acquired from a living rat to calculate the ADC. In Fig. 3a, $^{23}$Na MR spectra are displayed for varying $b$-values. In Fig. 3b, the modeling of the MR signal amplitudes to Eq. [1] is shown. The measured water ADC values of 0.83 and 0.51 $\mu$m$^2$/ms for living and dead rats are in agreement with previously published values (25).

Table 1
Summary of $^1H_2O$ Temperature and $^{23}Na^+$ Diffusion, $T_1$, and $T_2$ MR Measurements

| | $n$ | Average | Average error | Standard deviation |
|---|---|---|---|---|
| $S(b_1)$/noise | 18 | 7 | | 3 |
| Alive | | | | |
| ADC ($\mu$m$^2$/ms) | 18 | 1.15 | 0.09 | 0.13 |
| $T_1$ (ms) | 16 | 40 | 4 | 5 |
| $T_2$ (ms) | 16 | 34 | 2 | 2 |
| Dead | | | | |
| ADC ($\mu$m$^2$/ms) | 7 | 0.33 | 0.07 | 0.06 |
| $T_1$ (ms) | 6 | 35 | 5 | 4 |
| $T_2$ (ms) | 6 | 30 | 3 | 3 |

*Note.* Average $^{23}$Na MR time-domain signal-to-noise ratio at the first (smallest) $b$-value measured and $^{23}Na^+$ ADC, $T_1$, and $T_2$ in rat brain at 37 ± 2°C are given. The second column contains the average of the estimated error per measurement, and the third column represents the interanimal standard deviation of the measurements. The signal-to-noise ratio was determined by dividing the estimated amplitude of the time domain signal at the first (lowest) $b$-value by the standard deviation of the last 100 data points, representative of noise, in the free induction decay.

## DISCUSSION

Numerous theoretical discussions concerning the diffusion of water in mammalian tissues invoke reference to diffusion in the intracellular and extracellular spaces. Our interest in the sodium diffusion measurement is to gain insight, by inference, about the compartment specific displacement motion of water. Compartment selective (or specific) MR-active markers are useful in this regard because it is difficult to resolve the water MR signal from intracellular and extracellular environments. For example, Silva et al. (7) used intracerebroventricular infusions of

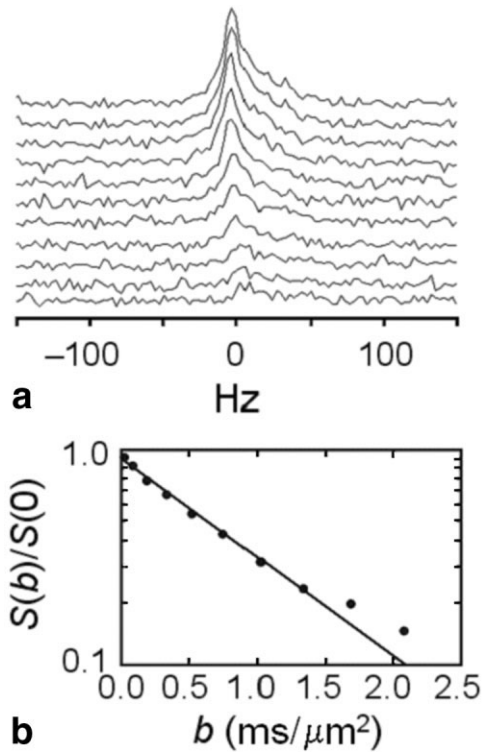


FIG. 3. **a**. Ten unfiltered spectra taken at $b$-values of 0.023, 0.086, 0.190, 0.336, 0.523, 0.752, 1.021, 1.332, 1.685, and 2.078 ms/$\mu$m$^2$. **b**. Estimated amplitudes of the time-domain data as a function of $b$-value, modeled (solid line) to a single exponential decay.

compartment-specific contrast agents to reduce $T_2$ in the extracellular space. The diffusion MR signal was collected at echo times long enough that none of the signal from the extracellular space was expected to remain. This provided a measure of water signal from the intracellular space. Extracellular water ADC was then deduced from the difference between intracellular water ADC and the overall (intracellular and extracellular) water ADC, using literature values for water content in each compartment.

In another example, our laboratory employed a series of $^{1}H$ or $^{19}F$ MR-active extracellular specific/selective markers to gain insight into the diffusion properties of this compartment (25,26). Two obvious caveats with interpretation of data from experiments of this type concern difficulties in quantifying/validating the degree of compartment specificity/selectivity in vivo and in accounting for specific and nonspecific binding of a particular marker to cellular membranes and other macromolecular entities. While the former issue can be difficult to resolve with in vivo systems in normal physiologic status, it is exacerbated with injured tissues (e.g., stroke) for which compartmental integrity may be compromised. The latter issue makes inferential assessment of compartmental water diffusion properties less firm, as the specific and nonspecific binding of a particular marker (interpreted as a hindrance and restriction to diffusion) is assuredly different from that for water. Presumably, this problem is most prevalent with low concentration markers for which the bound species become an appreciable fraction of the observed molecules.

Sodium concentration in the extracellular space, which composes roughly 20% of the brain tissue, is approximately 140 mM, while sodium concentration in the intracellular space is roughly 10 mM. Therefore, roughly 80% of the $^{23}Na$ signal (without diffusion weighting and assuming that relaxation times are similar in both spaces) is from the high concentration of $Na^+$ residing in the extracellular space. This is the reverse of the water compartmental distribution, which is about 80% intracellular. Thus, signal from water and sodium primarily arises from the intracellular and extracellular spaces, respectively, and both water and sodium are sufficiently concentrated that putative specific and nonspecific binding sites affect only a small fraction of the total population. Furthermore, at 37°C both water and aqueous $Na^+$ have similar free diffusion coefficients. We measured water and $Na^+$ $D^{free}$ in a phantom at 37°C to be 3 and 1.9 $\mu m^2$/ms, respectively. (This agrees with published $Na^+$ $D^{free}$ measured at similar temperatures (13)). Thus, water and $Na^+$ are rather equivalent diffusion probes of local environment.

The root mean squared molecular displacement along one dimension $\langle x^2 \rangle^{1/2}$ is related to the diffusion coefficient through the Einstein equation

$$\langle x^2 \rangle^{1/2} = \sqrt{2 \cdot D_{app} \cdot t_{diff}}, \quad [6]$$

for which $D_{app}$ is the apparent "free" diffusion coefficient (which differs from the true diffusion coefficient due to hindrances in displacement, which can be treated as an apparent viscosity). Substituting ADC for $D_{app}$, we apply the expression here to provide a rough estimate of $Na^+$ displacements in tissue. For the sine-shape gradients used in this experiment, $t_{diff} = \Delta - \delta/4$ (see the last term in Eq. [3]). Given the experimental conditions described for this study, $\langle x^2 \rangle^{1/2}$ for $Na^+$ is ~5 $\mu m$. This value is sufficiently large that a significant fraction of both intracellular and extracellular sodium ions must encounter cell membranes. Extracellular $Na^+$, however, is never wholly confined to any specific region as the extracellular space is a highly tortuous but connected compartment. In contrast, assuming that negligible sodium exchanges across the cell membrane during $t_{diff}$, intracellular $Na^+$ displacement is restricted to space within the cell.

Postmortem data suggest that $Na^+$ diffusion measurements provide a reasonable representation of water diffusion. Upon death, ion pump activity ceases. The fraction of sodium that is pumped across the membrane during the diffusion time is very small (well under 0.1% during the diffusion times used (27)). Thus, cessation of pump activity alone should have no effect on the MR-measured ADC. Cessation of pump activity causes the breakdown of ion gradients and influx of extracellular $Na^+$ into cells. As a result, $Na^+$ redistributes to equal concentrations in the intracellular and extracellular compartments, placing ~80% of $Na^+$ in the intracellular space. This partitioning is identical to that of water. Under these circumstances, the brain $Na^+$ ADC is 0.33 ± 0.06 $\mu m^2$/ms, which is 17% of $Na^+$ $D^{free}$ at body temperature. In a similar manner, the water ADC after death is 17% of water $D^{free}$. The identical reductions in the $Na^+$ and water ADC values relative to the corresponding $D^{free}$ values suggest that $Na^+$ is a faithful surrogate for examining biophysical influences on the water ADC in tissue and that the difference in ADC/$D^{free}$ ratios observed between $Na^+$ and water in living brain are due to differences in the biophysical properties of the intracellular and extracellular spaces.

In living brain, $Na^+$ ADC is 61% the aqueous $Na^+$ free diffusion coefficient at 37°C (1.15 versus 1.9 $\mu m^2$/ms). The corresponding reduction in brain water ADC compared to free diffusion at 37°C is 28% (0.83 versus 3 $\mu m^2$/ms). This suggests that the extracellular compartment presents a less hindered/restricted diffusion environment than does the intracellular compartment. More specifically, by inference, we would expect the water ADC of the extracellular space to be roughly twice that of the intracellular space.

This is consistent with the analysis of Silva et al. (7), who reported compartment-specific water ADCs in rat brain in vivo that differed by roughly a factor of 2, 0.7 and 1.6 $\mu m^2$/ms, respectively, for intracellular and extracellular compartments. However, this prediction is quantitatively different from that of an earlier report from our lab, for which the diffusion of exogenously administered 2-fluorodeoxyglucose-6-phosphate was found to be equivalent in these two compartments. This difference may reflect the marker-specific issues discussed above.

With regard to changes in $Na^+$ diffusion after the death of the animal, physiologic changes besides the loss of ion balance complicate extrapolation of these data to living tissue. Changes in the diffusivities of intracellular-specific compounds have been observed after death (15,26,28), and similar changes likely take place in the extracellular space. Therefore, while the observed convergence of the $Na^+$ and water ADC/$D^{free}$ ratios in dead tissue validates that $Na^+$ and water ADC values are similarly influenced by biophysical structural and dynamic features, values obtained from tissue postmortem do not mirror ADC values in living

tissue. Thus, although the majority of $Na^+$ is in the intracellular space after death, the ADC values cannot be taken to reflect those of the intracellular space in living tissue.

## CONCLUSION

A method for measuring the brain $Na^+$ ADC in living and recently deceased rats has been developed. The $Na^+$ ADC/$D^{free}$ ratio is 0.61, which is significantly higher than the corresponding ratio of 0.28 measured for water. After death, both the $Na^+$ and the water ADC/$D^{free}$ ratios decrease to the same value of 0.17. The ratios measured in the dead rats suggest that similar biophysical determinants govern $Na^+$ and water ADC values under conditions for which $Na^+$ and water share similar intra/extracellular partitioning. The difference between the ADC/$D^{free}$ ratios observed in the living rats is attributed to differences in homeostatic intra/extracellular partitioning for the two molecules, with diffusion in the extracellular environment being approximately twofold less hindered. Furthermore, if the ratio of extracellular/intracellular ADC values in vivo is approximately 2, then a simple volume shift of water to the intracellular space is not sufficient to account for the ~30–50% decrease in global tissue water ADC following injury.

## REFERENCES


1. Moseley ME, Cohen Y, Mintorovitch J, Chileuitt L, Shimizu H, Kucharczyk J, Wendland MF, Weinstein PR. Early detection of regional cerebral ischemia in cats: comparison of diffusion- and $T_2$-weighted MRI and spectroscopy. Magn Reson Med 1990;14:330–346.
2. Zhong J, Petroff O, Prichard J, Gore J. Barbiturate-reversible reduction of water diffusion coefficient in flurothyl-induced status epilepticus in rats. Magn Reson Med 1995;33:253–256.
3. Verhuel H, Balazs R, van der Sprendel J, Tulleken C, Nicolay K, Lookeren v. MRI characterization of diffusion coefficients in a rat spinal cord injury model. Brain Res 1993;618:203–212.
4. Ford J, Hackney D, Alsop D, Jara H, Joseph P, Hank C, Black P. MRI characterization of diffusion coefficients in a rat spinal cord injury model. Magn Reson Med 1994;31:488–494.
5. Hasegawa Y, Formato J, Latour L, Butierrez J, Liu K, Garcia J, Sotak C, Fisher M. Severe transient hpyoglycemia causes reversible change in the apparent diffusion coefficient of water. Stroke 1996;27:1648–1655.
6. Takano K, Latour L, Formato J, Carano R, Helmer K, Hasegawa Y, Sotak C, Fisher M. The role of spreading depression in focal ischemia evaluated by diffusion mapping. Ann Neurol 1996;39:308–318.
7. Silva MD, Omae T, Helmer K, Li F, Sotak C. Separating changes in the intra- and extracellular water apparent diffusion coefficient following focal cerebral ischemia in the rat brain. Magn Reson Med 2002;48:826–837.
8. Quirk JD, Bretthorst GL, Duong TQ, Snyder AZ, Springer CS, Ackerman JJH, Neil JJ. Equilibrium water exchange between the intra- and extracellular spaces of mammalian brain. Magn Reson Med 2003;50:493–499.
9. Syková E. The extracellular space in the CNS: Its regulation, volume and geometry in normal and pathological neuronal function. Neuroscientist 1997;3:28–41.
10. Neural Signaling. In: Augustine GJ, editor. Neuroscience. Second ed. Sunderland: Sinauer Associates, Inc.; 2001. p 50.
11. van der Veen J, van Gelderen P, Creyghton J, Bovée W. Diffusion in red blood cell suspensions: separation of the intracellular and extracellular NMR sodium signal. Magn Reson Med 1993;29:571–574.
12. Sehy JV, Ackerman JJH, Neil JJ. Apparent diffusion of water, ions, and small molecules in the *Xenopus* oocyte is consistent with Brownian displacement. Magn Reson Med 2002;48:42–51.
13. Lobo VM. Mutual diffusion coefficients in aqueous electrolyte solutions. Pure Appl Chem 1993;65:2613–2640.
14. Garwood M, DelaBarre L. The return of the frequency sweep: designing adiabatic pulses for contemporary NMR. J Mag Reson 2001;153:155–177.
15. Kroenke CD, Ackerman JJH, Neil JJ. Magnetic resonance measurement of tetramethylammonium diffusion in rat brain: comparison of magnetic resonance and ionophoresis *in vivo* diffusion measurements. Magn Reson Med 2003;50:717–726.
16. Corbett R, Laptook A, Weatherall P. Noninvasive measurements of human brain temperature using volume-localized proton magnetic resonance spectroscopy. J Cereb Blood Flow Metab 1997:363–369.
17. Price WS, Hayamizu K, Ide H, Arata Y. Strategies for diagnosing and alleviating artifactual attenuation associated with large gradient pulses in PGSE NMR diffusion measurements. J Magn Reson 1999:205–212.
18. Bretthorst GL. Bayesian analysis. III. Applications to NMR signal detection, model selection and parameter estimation J Magn Reson 1990; 88:571–595.
19. Stejskal EO, Tanner JE. Spin diffusion measurements: spin echoes in the presence of a time-dependent field gradient. J Chem Phys 1965;42: 288–292.
20. Karlicek RF, Jr., Lowe IJ. A modified pulsed gradient technique for measuring diffusion in the presence of large background gradients. J Magn Reson 1980;37:75–91.
21. Jaccard G, Wimperis S, Bodenhausen G. Multiple-quantum NMR spectroscopy of s=3/2 spins in isotropic phase: a new probe for multiexponential relaxation. J Chem Phys 1986;85:6282–6293.
22. Pekar J, Renshaw PF, Leigh JS. Selective detection of intracellular sodium by coherence-transfer NMR. J Magn Reson 1987;72:159–161.
23. Rooney WD, Springer CS. A comprehensive approach to the analysis and interpretation of the resonances of spins 3/2 from living systems. NMR Biomed 1991;4:209–226.
24. Reddy R, Bolinger L, Shinnar M, Noyszewski E, Leigh JS. Detection of residual quadrupolar interaction in human skeletal muscle and brain in vivo via multiple quantum filtered sodium NMR spectra. Magn Reson Med 1995;33:134–139.
25. Duong TQ, Sehy JV, Yablonskiy D, Snider BJ, Ackerman JJH, Neil JJ. Extracellular apparent diffusion in rat brain. Magn Reson Med 2001; 45):801–810.
26. Duong TQ, Ackerman JJH, Ying HS, Neil JJ. Evaluation of extra- and intracellular apparent diffusion in normal and globally ischemic rat brain via $^{19}F$ NMR. Magn Reson Med 1998;40:1–13.
27. Siesjö BK. Cellular work in the brain. brain energy metabolism. New York: Wiley; 1978. p 39–40.
28. Neil JJ, Duong TQ, Ackerman JJH. Evaluation of intracellular diffusion in normal and globally-ischemic rat brain via 133Cs NMR. Magn Reson Med 1996;35:329–335.